

## Annealing Texture Evolution of Ti-IF Steel during Batch Annealing

Jing Shi, Xianjin Wang

Material Science and Engineering School, University of Science and Technology Beijing, Beijing 100083, China

(Received 1998-04-15)

**Abstract:** Texture development and recrystallization behavior of Ti-IF steel during Batch Annealing (BA) were investigated with X-ray diffraction and EBSP in lab, and the results were compared with research work on continuous annealing (CA) with rapid heating rate. The basic tendencies are similar that early nucleation takes place in <111>/ND fibers, <110>/RD fibers are consumed at the end of recrystallization, and <111>/ND texture dominates over annealing texture. However, the detailed texture transformation during batch annealing is different and somewhat more complicated than that in rapid-heating process. Moreover, misorientation plays an important role in texture transformation of BA. In addition, the results of EBSP are consistent with that of ODF well.

**Key words:** Ti-IF steel; texture; batch annealing; X-ray diffraction; EBSP

$r_m$  value determined mainly by the textures of sheets steels is an important index to evaluate deep drawability of sheets, and strong {111} texture and weak {001} texture result in high  $r_m$  value [1]. Interstitial Free (IF) steels are distinguished from other steels with respect to the absence of carbon and nitrogen atom in  $\alpha$ - iron matrix, and it is the main factor contributing to its very narrow and intense {111} recrystallization texture and its high  $r_m$  value.

With the development of texture analysis techniques such as X-ray diffraction and EBSP, many researchers [2,4,7,9] have investigated the physical mechanisms of development of strong {111} recrystallization texture in IF steels. Nevertheless, most of the work deals with normal recrystallization process and/or continuous annealing, and there is relatively less research on the texture evolution of IF steels during batch annealing process. The present paper is to investigate texture development in Ti-IF steel during batch annealing process, and find its own characteristics.

### 1 Experimental

The experimental material is a typical cold rolled Ti-IF steel obtained in industrial production, and its chemical composition (mass fraction in %) is: C, 0.003 5; N, 0.002 8; S, 0.004 1; Ti, 0.076; Mn, 0.17; P, 0.01 and Nb, < 0.01. Steelmaking was done at a steelmaking work of Baotou Iron & Steel Corporation.

The material was melted in a 300 t BOF with further treatment in an RH degasser and cast on continuous casters. Hot rolling was done on a continuous wide strip mill, and cold rolling was carried out on a 5-stand mill with a cold reduction rate of 77%.

BA simulation was carried out in lab. For recrystallization behavior research of BA process, the samples were heated to various temperatures in a gas-protecting furnace at a rate of 50°C/h (typical to pure H<sub>2</sub> BA production) with different soaking time if necessary, and then quenched in water. In addition, the set highest temperature used here was 710°C that is a typical control temperature of batch annealing process. The number of quenched samples and the corresponding annealing conditions are listed in table 1.

The development of recrystallization was investigated mainly by Vickers hardness measurement and

Table 1 Batch annealing conditions of quenched samples

No.	Annealing condition	No.	Annealing condition
1	as cold-rolled	8	quenched at 710°C
2	quenched at 600°C	9	quenched at 710°C + 10 min
3	quenched at 620°C	10	quenched at 710°C + 20 min
4	quenched at 640°C	11	quenched at 710°C + 40 min
5	quenched at 660°C	12	quenched at 710°C + 1 h
6	quenched at 680°C	13	quenched at 710°C + 2 h
7	quenched at 700°C	14	quenched at 710°C + 4 h

SEM. The overall texture was measured by X-ray diffraction on Rigaku 2038, and the orientation distribution function (ODF) computed from the three incomplete pole figures  $\{110\}$ ,  $\{200\}$ , and  $\{112\}$ . The EBSP technique was also used to measure the orientation of grains in typical fields for some samples. In the most case, EBSP was performed at equal interval within a fixed observation field, but the orientation of individual grains also measured if necessary.

## 2 Results and discussion

### 2.1 ODF analysis of texture development

**Figure 1** shows the Vickers hardness evolution of the quenched samples above. From the figure, the start of recrystallization can be determined by a sharp drop in hardness. Meanwhile, the hardness decreased obviously before recrystallization owing to the long history of recovery. In this way, it is said recrystallization begin at the temperature between 640 and 660°C after heating at 50°C/h. and the samples before temper-

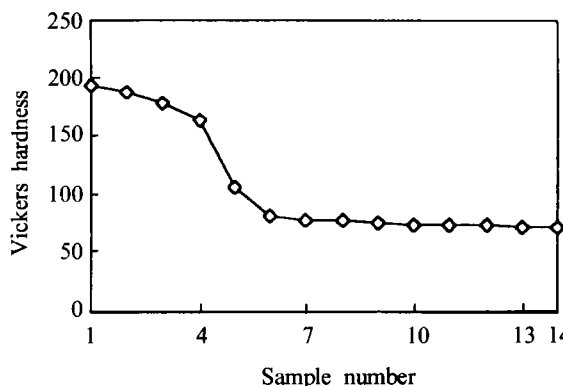


Figure 1 Hardness of quenched samples

ature reaches 660°C in this experiment are in recovery. The primary recrystallization is completed at 680°C, and then recrystallized grains continue to grow.

**Figure 2** shows the development of  $\alpha$ -fiber and  $\gamma$ -fiber texture in some of the quenched samples. **Figure 3** shows the evolution of volume fraction of texture in BA process. The main texture components in cold-rolled sample are  $\{112\} <110>$ ,  $\{111\} <110>$  and  $\{001\} <001>$ , all of which are typical cold rolled texture of IF steels. Although the volume fraction of main texture components changes little in recovery, the intensity of some texture components such as  $\{113\} <110>$ ,  $\{114\} <110>$  increases, which accounts for the orientation of deformed grains is changeable during recovery. When annealing temperature reaches 660°C, about 70% of deformed grains have recrystallized, but overall  $\alpha$ - and  $\gamma$ -fiber textures only have a little change. Moreover, the primary recrystallization ends at 680°C.  $\{113\} <110>$  texture decreases sharply while  $\{111\} <143>$  reaches its peak, but a strong  $\{001\} <110>$  texture still exists. From the results of ODF at  $\phi=45^\circ$  section shown in **figure 4**, the strongest texture components do not lie on  $<111>/ND$  axis. With further progress of annealing,  $\{001\} - \{113\} <110>$  components continue to decrease and  $\{111\} <110>$  component increases dramatically. After the temperature reaches 710°C, the overall texture does not change much with the soaking time.

### 2.2 Microtexture analysis

From the hardness curve and ODF analysis results, it was found samples No. 4, 5, 6 were critical to the recrystallization texture research of BA, so these three samples were selected for further investigation by

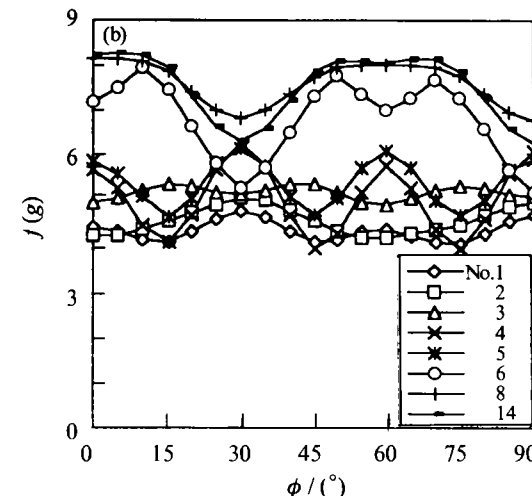
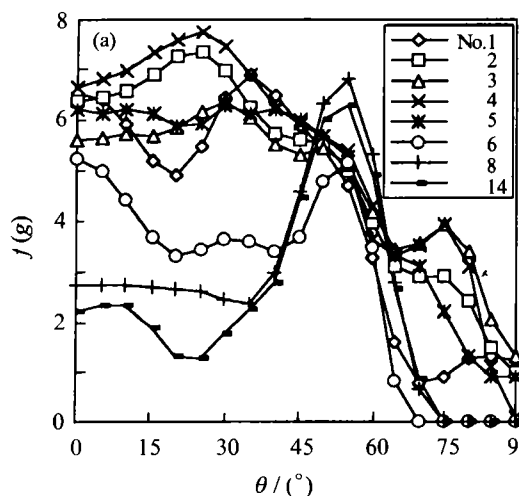


Figure 2 Development of overall textures in batch annealing of Ti-IF steel

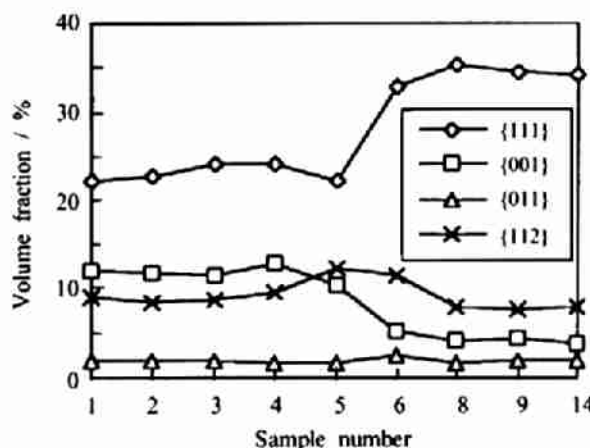


Figure 3 Evolution of volume fraction of different texture components in BA process

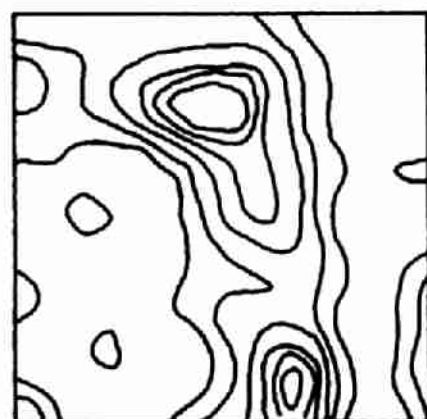


Figure 4  $\phi = 45^\circ$  ODF sections of sample No. 5 quenched at 680°C



Figure 5 SEM micrograph of samples No. 4, 5 and 6

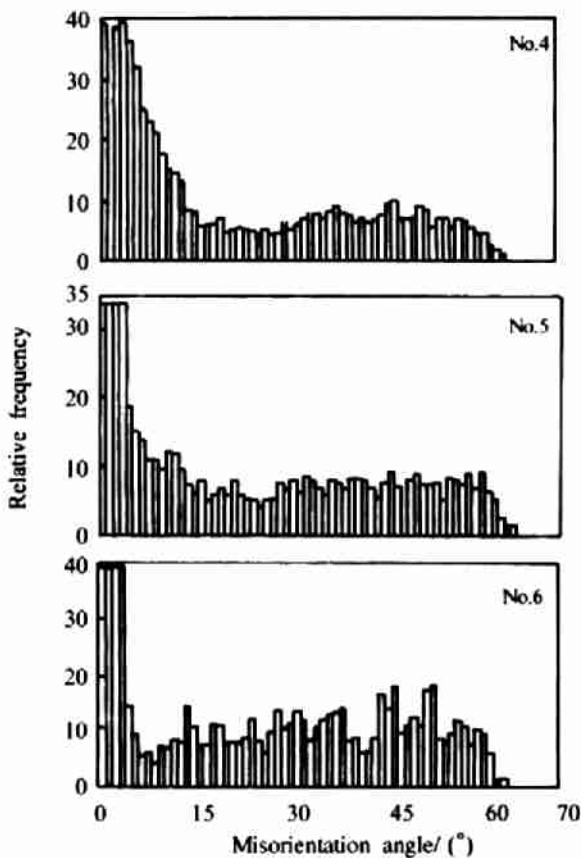


Figure 6 Misorientation distribution samples

means of EBSP. The SEM micrographs of samples No. 4, 5, 6 are shown in figure 5, it is shown sample No. 4 is fully recovered, No. 5 partially recrystallized and No. 6 fully recrystallized.

For each sample, EBSP was used to measure the grain orientation and misorientation in local fields at equal intervals. As for sample No. 5, EBSP was also performed only for the recrystallized grains. From figure 6, it is found the percentiles of small angle misorientation ( $<15^\circ$ ) in samples No. 4, 5, 6 are 55.3%, 45.6% and 34.1% respectively, which means the percentile decreases not only in recovery but also in primary recrystallization. In recovery, subgrain coalescence is main cause for the ratio reduction of small angle misorientation. Meanwhile, subgrain coalescence and consumption of deformed grains during primary recrystallization co-contribute to this tendency.

Figure 7(a-c) shows the inverse pole figures of normal plane of samples No. 4, 5, 6 respectively, and figure 7(d) shows the inverse pole figure of the recrystallized grains in No. 5. Although sample No. 5 is 70% recrystallized, its overall texture characteristics are similar to that of as cold rolled sample No. 4, and both of No. 4 and 5 are quite different from that of No. 6. This result is basically consistent with the results of ODF analysis as shown in figures 2 and 3. On the other hand, the texture of recrystallized grains in sample No. 5 is different from its overall texture, but similar to the texture of No. 6.

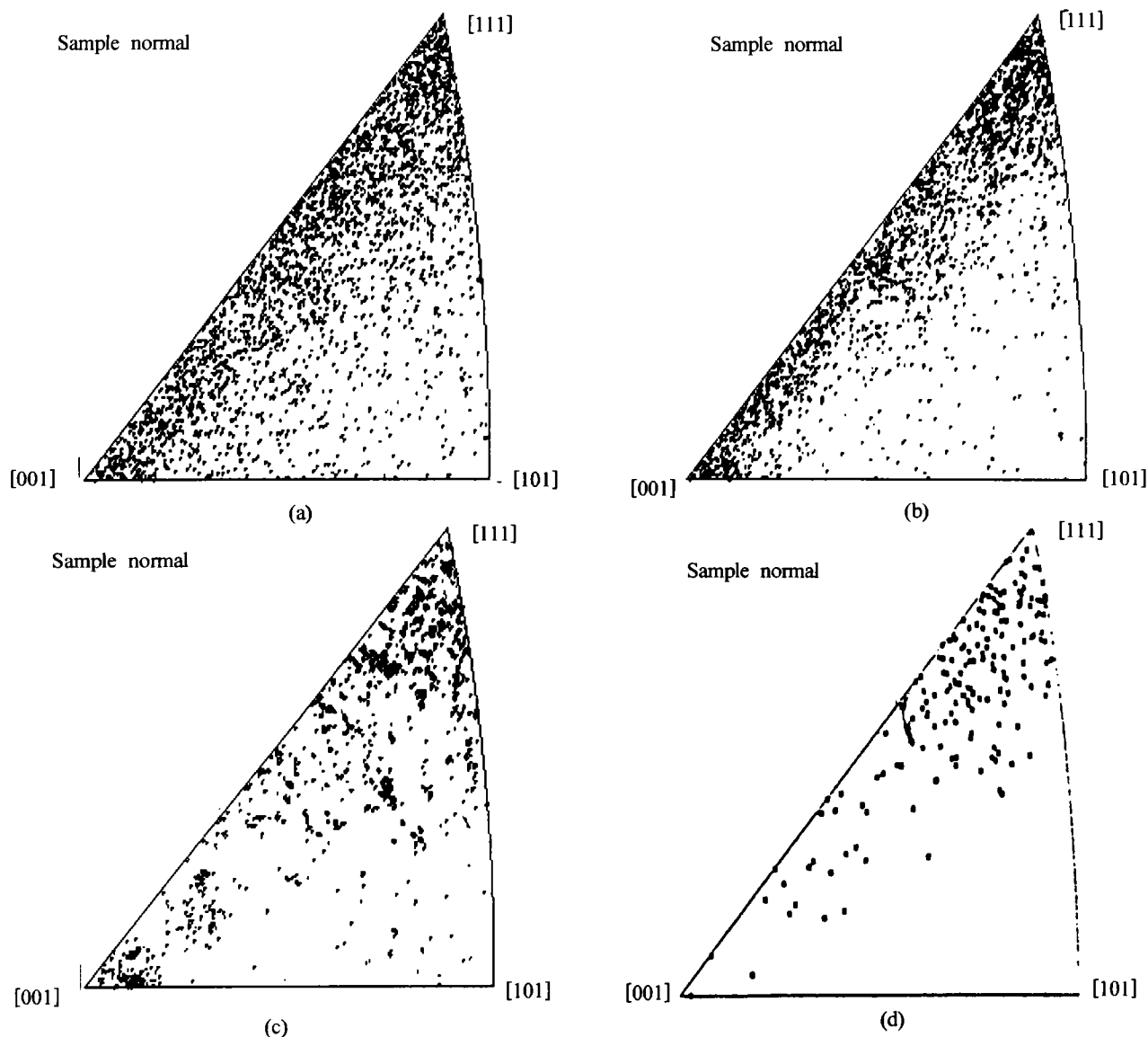


Figure 7 Inverse pole figures of normal plane of (a) No.4, (b) No.5, (c) No.6 and (d) recrystallized grains in No.5

In sample No. 4,  $\{111\}$  deformed fibers contain many subgrains less than  $2\mu\text{m}$  with large angle misorientation so that the EBSP pattern jumped in measuring process, while  $\{001\}$  fibers are very smooth and mostly misorientation in this fibers are less than  $5^\circ$ . Because the movement of large angle grain boundary is the main means of nucleation in IF steels, nucleation will firstly and mainly take place in  $\{111\}$  oriented deformed fibers. Nevertheless, nucleation could happen in heavily deformed metals by means of subgrain coalescence, so it is still possible that in a few cases nucleation takes place in other deformed fibers. In sample No. 5, most of the remaining deformed grains or subgrains are  $<110>/\text{RD}$  especially  $\{001\}<110>$  oriented, which consists with the idea that  $\alpha$  fiber are consumed in the end. In addition, there are a few  $\{001\}$  recrystallized grains in No. 5,

which mainly lie around  $\{001\}<110>$  deformed fiber, it can be inferred those  $\{001\}$  recrystallized grains are formed by amalgamation of  $\{001\}$  deformed subgrains with small angle misorientation. This phenomenon supports the existence of nucleation by subgrain coalescence in IF steels. Furthermore, the recrystallized  $\{001\}$  grains are generally smaller than other grains in No. 6, and the size of  $\{111\}$  grains is relatively larger than that of other grains. According to the simple model about grain growth [11], the  $\{001\}$  grains will continue to be consumed and the intensity of  $\{111\}$  grain will increase with the annealing process.

### 3 Conclusions

- (1) Batch annealing process can be categorized as

recovery, primary recrystallization, and grain growth. Compared with texture development in continuous annealing process, some  $\gamma$  fiber texture components change obviously in recovery while they hardly change in this stage during CA and the evolution of  $\gamma$  fiber texture is more complex in primary recrystallization. After primary recrystallization,  $\gamma$  fiber texture continues to change with the progress of batch annealing.

(2) The deformed fibers in IF steel contain many subgrains that are less than  $2\text{ }\mu\text{m}$ , and there always exists misorientation between subgrains. Large angle misorientations are much more in  $\gamma$  fibers than in other fibers, which makes nucleation easily take place in  $\gamma$  fibers and rarely in fibers with other orientations. Because of subgrain coalescence and grain consumption, the ratio of small angle misorientation decreases with the annealing process carried on.

(3) As for texture transformation during batch annealing, the orientation of new-formed nuclei inherits from their deformed matrix. In addition,  $\gamma$  fibers are preferably consumed first, and  $\gamma$  fibers especially  $\{001\}<110>$  are consumed in the end. Also, the results of EBSP consist with ODF analysis well.

## References

- 1 J F Held. Mechanical Working and Steel Processing IV. New York: American Institute of Mining, Metallurgical and Petroleum Engineers, 1965
- 2 B Hutchinson, E Lindh. International Forum for Physical Metallurgy of IF Steels. Tokyo, 1994. 127~140
- 3 I Gupta, *et al.* Metallurgy of Formable Vacuum-Degassed Interstitial-Free Steels. In: R Pradhan ed. Proc on Metallurgy of Vacuum-Degassed Steel Products. Indianapolis: TMS, 1989. 43~72
- 4 B Hutchinson. In: Proc of the 11th International Conf on Texture of Materials. Xi'an, 1996. 377~386
- 5 N Hashimoto, *et al.* In: Proc of the 11th International Conf on Texture of Materials. Xi'an, 1996. 429~434
- 6 D N Lee. In: Proc of the 11th International Conf on Texture of Materials. Xi'an, 1996. 503~508
- 7 D Vanderschueren, *et al.* In: Proc of the 11th International Conf on Texture of Materials. Xi'an, 1996. 1400~1405
- 8 R K Ray, *et al.* ISIJ International, 1994, 34(12): 927~942
- 9 Y Nagataki *et al.* ISIJ International, 1996, 36(4): 451~460
- 10 R K Ray, J J Jonas, R E Hook. International Materials Reviews, 1994, 39(4):
- 11 I L Dillamore, *et al.* Met Sci J, 1967(1): 49~54
- 12 X C Mi, B Y Kong. In: Proc of the 11th International Conf on Texture of Materials. Xi'an, 1996. 824~827

## Effects of Suspension Casting on Solidification Process of GCr15 Steel Ingot

Yan Yu, Qijie Zhai, Changhu Xing, Jinbao Chen, Hanqi Hu

Foundry Institution, University of Science and Technology Beijing, Beijing 100083, China

**Abstract:** The mechanism of inoculation in the case of suspension casting process has been studied through solidification kinetics. The effect of suspension casting process on temperature field, solidification rate, temperature gap of crystallization, effective distribution coefficient of solute and nucleation frequency during solidification process in steel ingot were discussed on the base of experiments. It has been found that the suspension casting process can increase both cooling rate and solidification rate of steel ingot, improve the temperature field and solute distribution, narrow the temperature gap of crystallization, and increase the nucleation frequency. Thus, the solidification time can be shorten, the solute can be well distributed, the shrinkage porosity can be reduced and the grain of crystallization can be fined.

**Key words:** suspension casting process; solidification kinetics; solidification rate; GCr15 Steel

[From *Journal of University of Science and Technology Beijing (in Chinese)*, 1998, 20(3): 264]